Comprehensive Assessment Method for Aero-Engine Performance and Risk Based on Emergency Operating

Shimeng Cui [1, a], Sirui Pan [2, b], and Zhenghong Han [1, c]

[1] COMAC Beiing Aircraft Technology Research Institute, China;

[2] School of Safety Science and Engineering, Civil Aviation University of China, China.

[a] cuishimeng@comac.cc, [b] psr1069342327@163.com, [c] hanzhenghong@comac.cc

Abstract. To improve the response performance of aircraft engines under emergency operating conditions, this article proposes a comprehensive performance and risk assessment method based on the release of limit protection parameters. The method introduces quantitative indicators such as limit exceedance rate and protection metrics with penalty functions to evaluate the increase in operational risk caused by limit relaxation. These risk metrics are integrated with performance improvement metrics into a unified relative performance index. To verify the feasibility of the method, simulation tests are conducted on a 90k-class turbofan engine model using the C-MAPSS platform under the flight condition of 25,000 feet and Mach 0.62. A Particle Swarm Optimization (PSO) algorithm is applied to determine the optimal limit release rate. Results demonstrate that engine acceleration response performance can be significantly enhanced while keeping the increased risk within acceptable bounds. This method provides a quantitative foundation for the design and validation of emergency control strategies for aircraft engines.

Keywords: Aero-Engine; emergency operation; limit protection; risk assessment.

1. Introduction

Aero-engine control is essential for ensuring thrust response and maintaining operational safety [1]. It must simultaneously achieve both power management and constraint management objectives. Striking a balance between safety and performance has long been a central challenge in aero-engine control design.

In the 1989 crash of United Airlines Flight 232 in Sioux City, the aircraft lost all hydraulic control surfaces. The flight crew attempted to control the aircraft using the remaining two engines, aiming for an emergency landing in Sioux City, Iowa. However, due to the conservative design of the aero-engine control system, it failed to provide sufficiently fast dynamic response under emergency conditions, which ultimately contributed to the accident [2].

Following the incident, NASA initiated the Propulsion Controlled Aircraft (PCA) program [3], aiming to enable aircraft to land safely by precisely controlling engine thrust without relying on hydraulic systems. Litt et al. [4] noted that traditional aero-engine control strategies result in slow engine response, which is inadequate during emergencies. Their subsequent research [5] showed that relaxing the limits of protection parameters is a simple and effective way to enhance aero-engine responsiveness.

Since the redline limits of an aero-engine are artificially imposed based on material properties and aero-thermodynamic constraints [6], these limits can be further relaxed in life-threatening situations to improve performance. While this may reduce engine safety margins and service life, the gain in rapid acceleration could save passengers and the aircraft. Therefore, when designing Enhanced Engine Control strategies, it is reasonable to moderately relax constraint limits—provided that the performance gains and the associated operational risks are quantitatively assessed.

This article investigates the increase in operational risk due to the relaxation of protection parameter limits, proposes relevant quantitative indicators, and verifies their feasibility through theoretical analysis and simulation examples, including the use of a Comprehensive Relative Performance Index.

2. Operational Risk Assessment Method

During acceleration, the primary constraint types to be considered include temperature limits, acceleration limits, and stall margin limits. These constraints can be represented by the limit protection parameters: High-Pressure Turbine Outlet Temperature (T_{48}) and the ratio of Fuel Flow to Compressor Static Pressure (Φ).

Operational risk arises from limit exceedance, and the parameters associated with such exceedances can serve as indicators of risk. To quantitatively describe potential violations of protection parameters, the concept of *limit exceedance rate* is introduced, as defined in Equation (1)。

$$\xi_i^+ = \max[\left(y_i - y_{i.lim}\right)/\left(y_{i,lim} - y_{ei}\right),0] \qquad (1)$$

In the equation, y_i represents the current value of the limit protection parameter; the subscript e indicates the value of the parameter at steady state; and the subscript *lim* denotes the constraint limit of the protection parameter.

To characterize the overall performance improvement and risk increase throughout the transient process, the limit protection index parameter is used to quantify the risk. Therefore, the limit protection index parameter is defined as shown in Equation (2).

$$NE_i(t) = \int_0^t [(1 + P_{1,i}(\tau,\xi_i^+) + P_{2,i}(\xi_i^+))\max[(y_i(\tau) - y_{i,lim}),0]]d\tau \cdots\cdots\cdots\cdots\cdots (2)$$

In the equation, the function P_1 is the duration penalty coefficient, which means that the longer the constraint is exceeded, the greater the damage to the engine. At the same time, considering that frequent acceleration may occur under emergency conditions, P_1 is reset to zero each time the limit protection parameter falls back below the constraint value, and is recalculated upon the next exceedance to avoid integral saturation. After comprehensive consideration, the form of P_1 is defined as:

$$P_{1,i}\ t\ \xi_i^+ \ = p_{1,i} \qquad \xi_i^+) f_{1,i}(t - t_0), t_0 = \qquad {}_{\tau\le t} |t - \tau| \qquad \xi_i^+\ \tau\ = 0 \cdots\cdots\cdots (3)$$

The function $P2$ is the exceedance magnitude penalty coefficient, which means that the greater the amount by which the constraint is exceeded, the more severe the damage to the engine. After comprehensive consideration, the form of $P2$ is defined as:

$$P_{2,i} = p_{2,i} f_{2,i}(\xi_i^+) \cdots\cdots\cdots\cdots\cdots\cdots\cdots\cdots\cdots\cdots\cdots\cdots (4)$$

In Equations (3) and (4) above, p_1 and p_2 are freely selectable parameters, and f_1 and f_2 are positively correlated functions. Since the degradation of aero-engine life increases exponentially with rising temperature and stress, while the effect of time can be approximately considered as linearly increasing [7], f_1 and f_2 are defined in the following form:

$$\begin{aligned} f_1(x) &= x \\ f_2(x) &= e^x \end{aligned} \cdots\cdots\cdots\cdots\cdots\cdots\cdots\cdots\cdots\cdots\cdots\cdots\cdots (5)$$

For the case of actively releasing the constraint limit of a protection parameter, the release rate r is defined. This variable is used to calculate the relaxed constraint value, and its specific value is determined by the designer. The relaxed limit protection constraint is defined as follows:

$$\overline{y}_i' = \overline{y}_i(1 + r_i) \qquad (6)$$

In the equation, $\overline{y}_i'$ represents the relaxed constraint value, and $\overline{y}_i$ is the original constraint value.

3. Comprehensive Relative Performance Index

To enable a cross-comparison of the trade-off between risk and benefit under different release rates, a relative metric must be constructed. Considering that the performance benefit is characterized based on fan speed, while the risk is characterized by the corresponding limit protection parameters, there exists a magnitude disparity between them. Therefore, to effectively compare risk and benefit, it is necessary to normalize each parameter against its respective reference value.

The Comprehensive Relative Profit J_{Po}, Comprehensive Relative Risk J_{NE}, and Comprehensive Relative Performance Index J are proposed and defined as shown in Equation (7):

$$\begin{aligned} J_{Po}(t) &= \frac{Po(t)-Po_{\min}(t)}{Po_{\max}(t)-Po_{\min}(t)} \\ J_{NE,i}(t) &= \frac{NE_i(t)-NE_{\min,i}(t)}{NE_{\max,i}(t)-NE_{\min,i}(t)} \\ J(t) &= J_{Po}(t)-\sum \alpha_i J_{Ne,i}(t) \end{aligned} \tag{7}$$

In the equation, the subscript min indicates the result obtained when the design constraint value is used (r=0), while the subscript max represents the result obtained when no limit protection measures are applied (r=∞). α_i denotes the weight representing the relative importance of each type of risk to the overall operational risk of the aero-engine, and it satisfies $\sum \alpha_i = 1$.

When t is taken as the end time of the acceleration process, t_{final}, it represents the comprehensive performance over the entire acceleration phase.

According to the definition of the Comprehensive Relative Performance Index in Equation (7), when the limit protection parameter release strategy takes the two extreme boundary cases—no release and full release —both J_{Po} and J_{NE} are equal to 0 in the former case, resulting in J = 0; and both J_{Po} and J_{NE} are equal to 1 in the latter case, which also yields J = 0 after computation. This definition conforms to the design expectation of balancing risk and benefit.

As the release rate r increases and remains constant throughout the entire acceleration transition, the performance improves and constraint limits are exceeded. However, since the performance benefit outweighs the associated risk, the rate of change of J with respect to r is positive, and the Comprehensive Relative Performance Index $J(t_{final})$ increases. Later, due to diminishing marginal returns, the benefit gained from relaxing the protection constraints becomes smaller than the resulting risk increase. As a result, the rate of change of $J(t_{final})$ with respect to r becomes negative, and $J(t_{final})$ begins to decrease. Based on this analysis, it can be expected that $J(t_{final})$ is a function that starts from 0, increases first, then decreases, and eventually drops back to 0. In general, there exists a maximum value of $J(t_{final})$, corresponding to an optimal release rate r_{best}.

In summary, by solving the optimization problem (8), the optimal release rate r_{best}.can be determined.

$$\max \quad J(t_{final}) \tag{8}$$

4. Simulation Analysis

The simulation analysis in this article adopts the linearized model of a 90,000-pound class two-spool turbofan engine under the operating condition of 25,000 feet altitude and Mach 0.62 (FC07), based on the Commercial Modular Aero-Propulsion System Simulation (C-MAPSS) platform [8,9].

The increment constraints are defined as [9]:

$$\begin{cases} \Delta T_{48} \quad (y_2 \le \bar{y}_2 = 600^{\circ}\,\mathrm{R} = 333.33\ \mathrm{K}) \\ \Delta \Phi \quad (y_3 \ge \bar{y}_3 = 18\ \mathrm{pps/psi} = 1.184\ \mathrm{kg/(s\cdot kPa)}) \end{cases} \tag{12}$$

Fig. 1 shows the schematic of the Min-Max selection structure for the aero-engine with a sliding mode controller used in this article.

The selected sliding mode control law is:

$$u_{ri} = -\frac{1}{\Theta_i}(G_i(Ax+Bu)+\eta_i sign(s_i))$$
$$s_i = y_i - \overline{y}_i, i=1,2,3 \quad (13)$$

In the equation, $\eta_1 = 15$ and $\eta_i |\Theta_i| = 20, i = 2,3$ [9]。

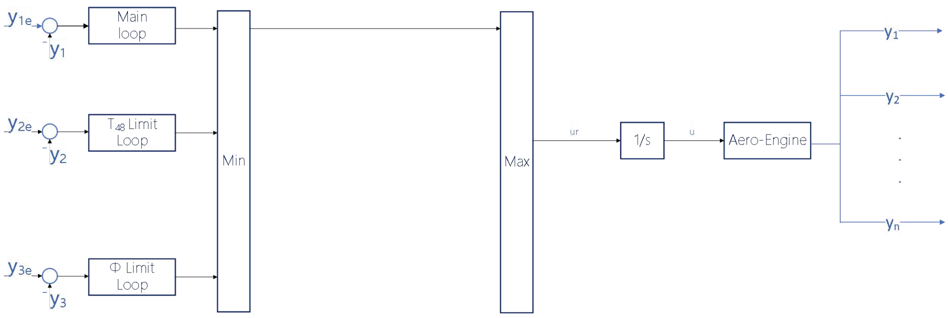

Fig. 1 Aero-engine Min-Max Selection Architecture with Sliding Mode Controller

To simulate an emergency scenario requiring an increase in engine fan speed, the fan speed setpoint is set to $\Delta N_1 = 340$ rpm at simulation time 0 s, with the simulation running for 3 seconds.

Release rates of *r*=0 and *r*=∞ are selected respectively, with α_1 and α_2 both set to 0.5, in order to obtain the parameter values with "min" and "max" subscripts in Equation (7). The results are as follows:

$Po_{min}(t_{final})$=850.44， $NE_{min,T48}(t_{final})$=0， $NE_{min,\Phi}(t_{final})$=0；

$Po_{max}(t_{final})$=902.03， $NE_{max,T48}(t_{final})$=280.28， $NE_{max,\Phi}(t_{final})$=17.35。

A total of 46 simulations were conducted with the release rate *r* set to [5%,6%,7%,…,50%]. The simulation results are shown in Fig. 2.

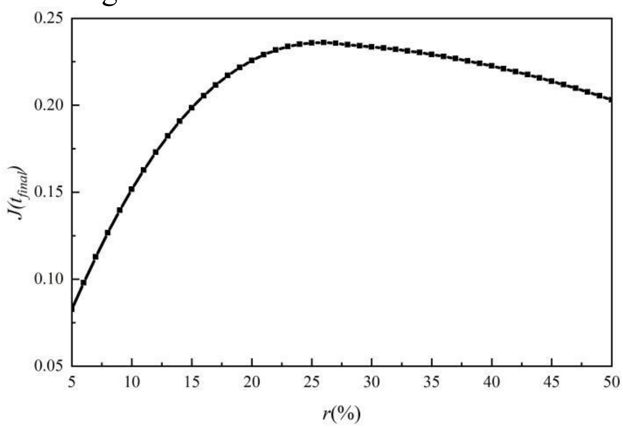

Fig. 2 Plot of changes in relative composite performance indicators corresponding to different release rates

$J(t_{final})$ exhibits an increasing-then-decreasing trend.

The Particle Swarm Optimization (PSO) algorithm is used to solve the optimization problem (8), resulting in an optimal release rate of r_{3best}=25.8228%, which is consistent with the peak of $J(t_{final})$ observed in the simulation sweep between 25% and 26%.

As shown in Fig. 3 and Tab. 2, the performance characterization time parameters all improved to 0.0827 s, 0.1559 s, and 0.1560 s respectively, with corresponding improvement rates of 16.97%, 17.19%, and 12.78%. The exceedance levels of the limit protection parameters were also controlled within acceptable ranges, demonstrating the effectiveness of the Comprehensive Relative Performance Index.

Table 2. Summary of simulation results for optimal release rate

$J(t_{final})$	T_D (s)	T_R (s)	T_S (s)	ΔT_{48_MAX} (K)	$\Delta \Phi_{\_MAX}$ (kg/(s·kPa))
0.2360	0.4046	0.7508	1.0647	381.43	1.49

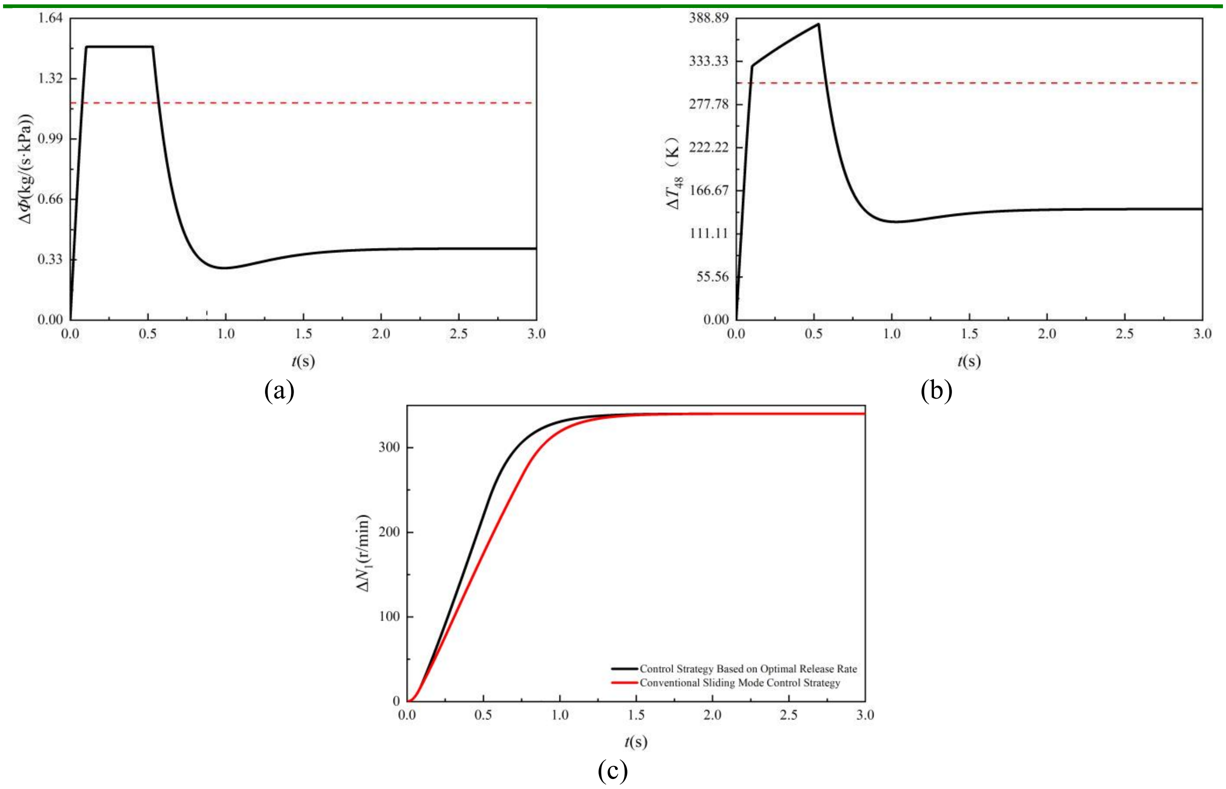

Fig. 3 Optimal release rate simulation result graph

5. Summary

This article conducted an in-depth study on the operational risk increase caused by the release of limit protection parameter constraints, proposed relevant quantitative indicators, and verified their feasibility through theoretical analysis and simulation examples.

The method for quantifying both performance and protection effectiveness was further refined to better characterize specific risks. A revised limit protection index was proposed by incorporating both the duration and magnitude of constraint violations. Based on this, risk escalation indicators and performance improvement indicators were normalized under boundary operating conditions, enabling cross-comparison between the two and ultimately forming the Comprehensive Relative Performance Index.

Multiple comparative simulations were performed on the C-MAPSS 90k engine under the FC07 operating condition. First, the boundary cases of the release rate were analyzed to determine key parameters of the Comprehensive Relative Performance Index. Then, a series of simulations with general release rates showed that the index exhibits a trend of increasing and then decreasing, with a clear maximum. The optimal release rate was determined by solving the optimization problem. At this release rate, the performance improved significantly compared to the conventional sliding mode control strategy. The performance characterization time parameters improved to 0.0827 s, 0.1559 s, and 0.1560 s, with improvement rates of 16.97%, 17.19%, and 12.78%, respectively. The increase in risk remained within a controllable range, with the maximum exceedance rate of limit protection parameters kept lower than the release rate. These results confirm that the Comprehensive Relative Performance Index effectively balances performance improvement with risk escalation.

References

[1] Csank J, May R, Litt J, et al. Control Design for a Generic Commercial Aircraft Engine. 46th AIAA/ASME/SAE/ASEE Joint Propulsion Conference & Exhibit, 2010.

[2] Aircraft Accident Report·United Airlines Flight232, McDonnell Douglas DC-10-10, Sioux Gateway Airport, Sioux City, Iowa, July 19, 1989. NATIONAL TRANSPORTATION SAFETY BOARD, 1989.

[3] Tucker T. Touchdown: The Development of Propulsion Controlled Aircraft at NASA Dryden. 1999.

[4] Litt J, Guo T H. Fast Thrust Response for Improved Flight/Engine Control under Emergency Conditions. AIAA Guidance, Navigation and Control Conference and Exhibit, 2008.

[5] Litt J, Frederick D, Guo T H. The Case for Intelligent Propulsion Control for Fast Engine Response. AIAA Infotech@Aerospace Conference, 2009.

[6] Yang S B, Wang X, Wang H N, et al. Sliding mode control with system constraints for aircraft engines. ISA Transactions, 2020, 98: 1-10.

[7] Litt J, Sharp L, Guo T H. A Risk Assessment Architecture for Enhanced Engine Operation. AIAA Infotech@Aerospace 2010, 2010.

[8] Richter H. Advanced Control of Turbofan Engines. New York, NY: Springer New York, 2012.

[9] Richter H. A multi-regulator sliding mode control strategy for output-constrained systems. Automatica, 2011, 47(10): 2251-2259.